Research Article

Validation and setting up quality control for characterization of aluminum alloys in non-ferrous fraction of auto-shredders

Maria A. Trancoso[1] · Carlos Nogueira[2] · Sandra Calisto[1]

Received: 7 May 2020 / Accepted: 17 September 2020 / Published online: 3 October 2020

Abstract
The improvement of recycling rates of metal waste, namely those of end-of life vehicles, is nowadays becoming imperative. Aluminum and its alloys are the main metal components in non-ferrous fraction of auto-shredders separated out after sampling. Silicon, Mg, Cu, Zn, Mn, Ti, Fe and Cr are alloying elements, which allowed the identification and differentiation of Al alloys. Flame Atomic Absorption Spectrometry was used for quantification after HCl-HNO_3 digestion, with the exception of Si, where HCl–HNO_3–HF–H_3BO_3 digestion was used. Performance characteristics of measurement procedures, namely analytical dynamic ranges, limits of detection and quantification, precision and trueness were evaluated and measurement uncertainty estimated by applying an approach based on precision and trueness validation studies and quality control data. Target values, for repeatability, intermediate precision, trueness (recovery) and measurement uncertainty, were specified to differentiate Al alloys based on their own fit-for-purpose. Metrological traceability of the measurements results of the alloying elements was established by using certified values of British Chemical Standard (BCS) of Al alloys, BCS nº 181/1, BCS Nº 268. BCS Nº 300 and Standard Reference Material of Al-base alloy, SRM 87. The quantification of Si, Mg, Cu, Zn, Mn, Ti, Fe and Cr in aluminum alloys from the non-ferrous fraction of automatic crushers was determined successfully through the validated procedures.

Keyword Aluminum alloys · Validation · Uncertainty · Traceability · Target · Intermediate precision · Recovery

Abbreviations

AA	Atomic absorption
BCS	British chemical standard
CQC	Calibration quality coefficients
CRM	Certified reference material
CS	Calibration standards solutions
D2	Deuterium lamp
DS^2	Difference of the squared residual standard deviations of linear and second order functions
ERM	European Reference Materials
FAAS	Flame atomic absorption spectrometry
IUPAC	International Union of Pure and Applied Chemistry
n.d.	Not detected
Max	Maximum
Min	Minimum
MU	Measurement uncertainty
NIST	National Institute of Standards and Technology
PTFE	Polytetrafluoroethylene
QC	Quality control standards solutions
SI	International System of Units
SRM	Standard Reference Material
TV	Testing value for linearity evaluation

List of symbols

A_j^{rel}	Relative amplitudes of j duplicate
B_c	Calibration blank (absorbance)
B_{dig}	Digestion blank (absorbance)

✉ Maria A. Trancoso, maria.trancoso@lneg.pt | [1]Unidade de Bioenergia e Biorrefinarias, Estrada do Paço do Lumiar, Laboratório Nacional de Energia e Geologia, LNEG, Ed. E – 1°, 1649-038 Lisboa, Portugal. [2]Unidade de Materiais para a Energia, Laboratório Nacional de Energia e Geologia, LNEG, Ed. C – 1°, 1649-038 Lisboa, Portugal.

SN Applied Sciences (2020) 2:1762 | https://doi.org/10.1007/s42452-020-03554-9

F One-sided critical value of the Fisher-Snedecor distribution ($p = 0.99$)
F_{dil} Dilution factor for the digestion solution in order to bracket the calibration curve.
K Coverage factor
P Probability of approximately 95%
m Mass of sample taken for analysis (g)
N Number of calibration data pairs
n Number of participants
R Recovery
$\overline{R}_{\gamma}$ Mean recovery from spiked digestion solutions
$\overline{R}_{CRM}$ Mean recovery estimated from CRM analysis
s Standard deviation (g/100 g)
$s\left(A_j^{rel}\right)$ Relative standard deviation of A_j^{rel}
s_{IP}^{rel} Relative standard deviation in intermediate precision consitions
$s_{IP(tg)}^{rel}$ Target value of s_{IP}^{rel}
s_{QC}^{rel} Relative standard deviation of QC
$s_{QC(tg)}^{rel}$ Target value of s_{QC}^{rel}
s_r^{rel} Relative standard deviation, in repeatability conditions
$s_{r(tg)}^{rel}$ Target value of s_r^{rel}
$s_{\overline{R}}$ Standard deviation of $\overline{R}$
s_{y1} Residual standard deviation for linear function (mg $L^{-1)}$
s_{y2} Residual standard deviation for second order function (mg L^{-1})
t_{cal} Significant statistic test
$u_c^{rel}(w)$ Relative combined standard uncertainty of w
$u\left(\overline{R}\right)$ Standard measurement uncertainty of $\overline{R}$
$u\left(s_{IP}^{rel}\right)$ Standard measurement uncertainty of s_{IP}^{rel}
$u\left(w_{CRM}\right)$ Standard measurement uncertainty of w_{CRM} (g/100 g)
$u\left(\overline{w}_{CRM}^{obs}\right)$ Standard measurement uncertainty of $\overline{w}_{CRM}^{obs}$ (g/100 g)
U Expanded uncertainty
U_{Δ} Expanded uncertainty of Δ (g/100 g)
V Volume of the sample digestion solution (mL)
w Mass fraction of the metal (g/100 g)
w_{CRM} Certified mass fraction of CRM (g/100 g)
$\overline{w}_{CRM}^{obs}$ Mean of observed results from CRM analysis (g/100 g)
y_i Absorbance value for ith standard solution
γ_{LOD} Limits of detection in the digestion solutions (mg L^{-1})
γ_{LOQ} Limit of quantification in the digestion solutions (mg L^{-1})
γ_M Mass concentration of the element on the digestion solution (mg L^{-1})
γ_{M+sp} Mass concentration of the element plus analyte spike on the digestion solution (mg L^{-1})
γ_{sp} Mass concentration of analyte spike added to the digestion solution (mg L^{-1})
γ_{QC} QC mass concentration (mg L^{-1})
$\hat{y}_i$ Absorbance of the standard concentration xi interpolated from the calibration function
Δ Difference between w_{CRM} and $\overline{w}_{CRM}^{obs}$ (g/100 g)

1 Introduction

Light alloys, namely aluminum and, more recently, magnesium alloys, have been progressively used in many equipment's such as vehicles, aiming reducing weight and fuel consumption. The driving forces for replacing classic alloys (namely those steel-based) for such new ones have been not only an economic but also an environmental task, trying to save resources and decreasing emissions [1–3]. The improvement of recycling rates of metal waste, namely those from end-of life vehicles, is nowadays becoming imperative because they constitute an important waste stream.

Aluminum and its alloys are the main metal components in non-ferrous fraction of auto-shredders, which also contains copper, brass, stainless steel, zinc and eventually magnesium. The use of light alloys in automotive applications, mainly aluminum but also magnesium, has been progressively increasing. Such alloys shall be recycled, at the end-of-life, due to environment and economic reasons, since recycling of aluminum provides much lower energy consumption than its extraction from primary resources. A major issue in recycling schemes is the separation of wrought and cast alloys, mainly based on the silicon content. Moreover, additional differentiation of alloys by the contents of some target elements would be advisable. Sorting aluminum alloys based on its chemical composition can be a reliable approach to improve efficiency and aluminum recycling rates in this type of waste [3]. Silicon, Mg, Cu, Zn, Mn, Ti, Fe and Cr are the relevant elements selected (alloying elements) to differentiate Al alloys. For instance, silicon is a good example of an alloying element for sorting Al alloys in non-ferrous auto-shredder fractions by its chemical content, since many alloys have different Si content [2].

In the project Shreddersort, an automated sorting technology was developed, allowing the separation of some Al alloy classes, based on two main techniques, the electromagnetic tensor spectroscopy (EMTS) and the laser induced breakdown spectroscopy (LIBS), as described elsewhere [1, 2]. As starting point for the technology development, a complete and accurate chemical analysis of the aluminum scrap was mandatory, in order to identify the

main Al alloy series present. Such identification was performed based on the content of specific elements, such as Si for differentiating cast and wrought alloys, as a first step. Identification of main series was achieved by the content of other elements. Examples are, for wrought alloys, the Mg content (in 5000 and 6000 series), the Mn content (in 3000 series) and the very low content of all the alloying metals in 1000 series. In cast alloys, besides de characteristic high Si content, the differentiation of some series was also possible, the most common being the 300 series from their copper content.

The experimental characterization plan was based on the collection of random and representative scrap samples from four vehicle recycling companies. Figure 1 shows Examples of shredder aluminium scraps. Non-ferrous fractions were collected by sampling and the materials screened and classified by classes, sub-classes, morphology and fragment size. After that physical analysis, metal pieces from each subclass were chemical characterized using flame atomic absorption spectrometry (FAAS) after appropriate acid digestions. An HCl–HNO_3 acid mixture for Mg, Cu, Zn, Mn, Ti, Fe and Cr analysis was used, as described further, while for Si analysis an adapted digestion with a HCl-HNO_3-HF mixture was used, followed by HF complexation using H_3BO_3 [4, 5]. This fluoric-boric acid matrix has no influence on the absorbance signal for Si, as previously studied [5].

Validation of the measurement procedure, metrological traceability and measurement uncertainty (MU) of the results are the key factors to ensure the quality of the chemical measurements. In according to the vocabulary of international metrology [6] validation is the verification, wherein the specified requirements are adequate for an intended. Metrological traceability is the property of a measurement result whereby the result can be related to a reference through a documented unbroken chain of calibrations, each contributing to the measurement uncertainty wherein MU is the non-negative parameter characterizing the dispersion of the quantity values being attributed to a measurand, based on the information used [6].

Nowadays, the validation of measurement procedures aims both the evaluation of the performance characteristics and the demonstration that those performances are suitable for the intended use of the results. A single validation approach to determine the metrological characteristic of the measurement procedures selected following Eurachem guidelines [7] for quantitative test for impurities, namely analytical dynamic ranges, calibration functions, limits of detection and quantification; stability control of the calibration functions; evaluation of contamination; matrix effects; precision and trueness. In addition, it was given special attention to measurement uncertainty, besides from MU not being a performance characteristic of a measurement procedure, but a property of the results obtained using that measurement procedure, the validation studies and quality control data comprising the entire analytical procedures. The main uncertainty components are trueness (recovery) and precision (reproducibility within the laboratory), which comprise the systematic and random and errors, respectively.

Precision component in intermediate conditions were calculated associating the repeatability standard deviation from duplicate analysis with ones obtained from the individual control charts of the quality control standards. The trueness component of the overall analytical procedure was obtained from the analysis of different CRM [8–10], namely BCS nº 181/1, BCS Nº 268, BCS Nº 300 and SRM87a).

Both measurement uncertainty and measurement traceability of the results give the metrological quality allowing comparability [11, 12]. To assess measurement

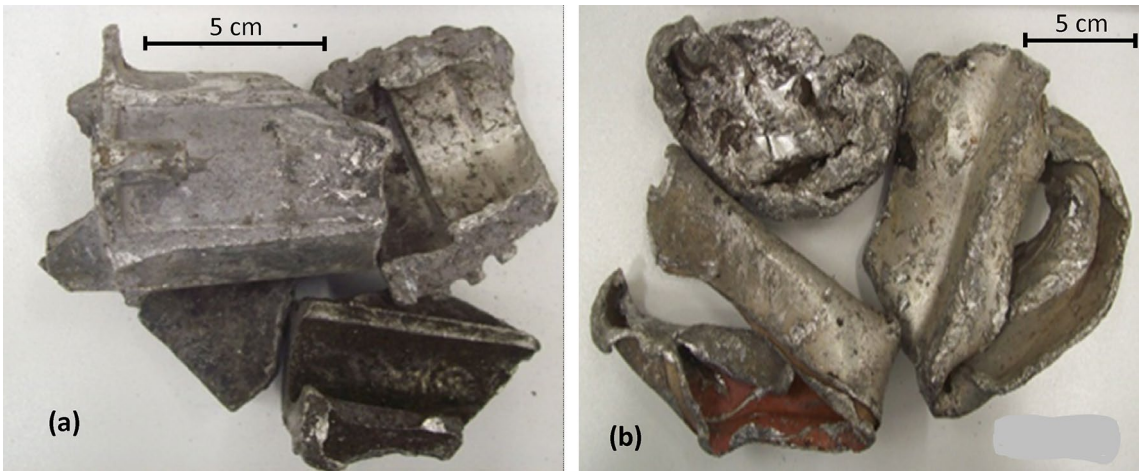

Fig. 1 Examples of shredder aluminium scraps: **a** cast fragments; **b** wrought fragments

uncertainty for their intended use in the field of this work, information for setting the target MU from regulation, specification or measurement quality requirements was not available. Target values for repeatability, intermediate precision, trueness (recovery) and uncertainty for Al alloys differentiation in non-ferrous fraction of auto-shredders were stated from their own fit-for-purpose. The selection of CRM either for target mass fraction or the matrix matching, contributes to the statement of metrological traceability.

The aim of this paper was to assess the performance characteristics of the measurement procedures used for the chemical characterization of aluminum alloys in non-ferrous fraction of auto-shredders and setting up quality control actions. Own fit-for-purposes were set for all performance characteristics of the analytical procedures providing reliable data for differentiating Al alloys.

2 Experimental

2.1 Materials and equipment

All the reagents were of analytical reagent grade from Merck (Darmstadt, Germany) and all solutions prepared using ultrapure water of 18 MΩ cm^{-1} resistivity, supplied from a Millipore Milli-Q water purification system (Millipore, Bedford, MA).

Calibration standard solutions, CS, were prepared from Certipur® reference standard solutions with 1000 mg L^{-1} for each metal from daily, quality control standard solutions, QC, were prepared just before put into use, spending independent reference standard solutions from Merck (Darmstadt, Germany). Merck solutions have metal contents traceable to the unit mg L^{-1} of the International System of Units (SI) checked through the analysis of the corresponding SRM produced by NIST of the USA.

The CRMs used were: 4% copper aluminum alloy, BCS nº 181/1, 5% silicon aluminum alloy, BCS nº 268, aluminum alloy BCS nº 300 from British Chemicals and a silicon-aluminum alloy, SRM 87a from the National Bureau of Standards.

All samples were dried into a Heraeus drying oven at 105 °C, after washing. A calibrated AT 200 Mettler balance was used for all weighing's. Volume measurements were taken using volumetric equipment of class A and As.

Alloying metals were determined by FAAS using a Solar 969 AA Spectrometer (Thermo Elemental, England) equipped with a deuterium lamp for the background correction, selecting each most intense line as manufacture recommendations [13]: Table 1 shows the optimized operational conditions. The instrument was operational whenever the absorbance of a standard solution did not differ more than 20% of the manufacturer´s recommended values [11, 12].

Calibrations were performed at six levels, including a calibration blank,B_c, covering the mass concentration ranges (Table 2). The CS and QC measurement solutions were prepared for Mg in HCl 0.5 mol L^{-1} solution containing 6 g L^{-1} of La_2O_3 as releasing agent minimizing oxyanion interferences. Iron and Mn were determined in HCl 0.5 mol L^{-1} solution with 50 mg L^{-1} of Ca to avoid chemical interferences [14]. In case of Cu, Zn, Si, Ti and Si the standards were prepared in 0.5 mol L^{-1} HNO_3 solution containing 2 g L^{-1} of KCl only for Si, Ti and Cr to overcome those ionization interferences. No matrix matching due to HF–H_3BO_3 acid was required, as previously studied [5]. Each absorbance values were the average of three absorbance readings with 3 s of integration time.

Table 1 Operational conditions for FAAS

Element	Wavelength (nm)	Lamp		Slit width (nm)	Background correction	Flame chemistry	Burner head (cm)
		current (mA)	% of maximum intensity				
Chromium	357.8	12	75	0.5	no	N_2O/C_2H_2–reducing	5
Copper	324.8	5	50	0.5	no	Air/C_2H_2–stoichiometric	10
Iron	248.3	15	75	0.2	yes (D2 lamp)	Air/C_2H_2–stoichiometric	10
Magnesium	285.1	4	75	0.5	no	Air/C_2H_2–stoichiometric	10
Manganese	279.5	12	75	0.2	no	Air/C_2H_2–stoichiometric	10
Silicon	251.5	15	75	0.5	yes (D2 lamp)	N_2O/C_2H_2–reducing	5
Titanium	365.3	15	75	0.5	no	N_2O/C_2H_2–reducing	5
Zinc	213.9	10	50	0.5	yes (D2 lamp)	Air/C_2H_2–stoichiometric	10

Table 2 Metrological performance characteristics of calibration functions

Element	Concentration range (mg L^{-1})	Absorbance range	*TV*	*CQC*	γ_{LoD} (mg L^{-1})	γ_{LoQ} (mg L^{-1})
Chromium[a]	0.1–2	0.01 – 0.21	7.4	0.01	0.03	0.09
Copper[a]	0.05–1	0.01 – 0.18	0.4	0.01	0.006	0.02
Iron[a]	0.2–2	0.01 – 0.20	3	0.03	0.07	0.2
Magnesium[b]	0.01–0.2	0.02 – 0.30	35	0.01	0.001	0.004
Manganese[a]	0.1–0.6	0.01 – 0.15	3.7	0.02	0.02	0.05
Silicon[a]	10–80	0.03 – 0.27	1.2	0.02	1.7	6
Titanium[b]	2–25	0.02 – 0.12	23	0.01	0.8	2
Zinc[a]	0.02–0.4	0.02 – 0.29	7.6	0.02	0.009	0.03

TV Testing value for linearity evaluation $\left(TV = DS^2/s_{y2}^2\right)$, with $DS^2 = (N-2)s_{y1}^2 - (N-3)s_{y2}^2$ [15, 16]

$CQC = \sqrt{\frac{\sum_i^N \left(\frac{(y_i - \hat{y}_i)}{y_i}\right)^2}{N-1}}$ [17, 18]

[a]First-order calibration function

[b]Second-order calibration function

Fig. 2 Examples of samples of smaller fragments suitable for analysis, obtained from raw fragments (as depicted in Fig. 1) after surface cleaning, cutting/drilling until average size lower than 0.5 cm

2.2 Sample preparation and acid digestions

To avoid chemical contamination, mechanically, the fragment surfaces of the samples, were cleaned, cuted and drilled in smaller fragments suitable for analysis, as shown in Fig. 2. Afterwards, it was washed all samples and CRM with ethanol followed by ultrapure water and drying at 105ºC before acid decomposition. Two different acid mixtures for solubilisation procedures were considered due to the different behaviour of the elements in acids. An HCl–HNO_3 acid mixture for Mg, Cu, Zn, Mn, Ti, Fe and Cr analysis and HCl–HNO_3–HF mixture followed by HF complexation using H_3BO_3 for silicon [4, 5]. Following those experimental measurement procedures, perform blank reagent, QC, CRM in duplicate sets.

Figure 2

2.2.1 Hydrochloric–nitric acid digestion

Samples and CRM's (≈ 0.5 g) were weighed into a 250 ml beaker to which 20 mL of 6 mol L^{-1} HCl solution was slowly added, followed by 5 ml of HNO_3. Those mixtures were gradually heated on a hot plate. Temperature was increased until mixtures gently boiled for 3–5 min to expel the nitrous vapours. After cooling, the solution was transferred into 100 ml volumetric flask with ultrapure water and diluted to the mark. It was let settle overnight and whenever necessary the mixture was filtered before atomic absorption measurements.

2.2.2 Hydrochloric–fluorohydric—nitric–boric acid mixture digestion

About 0.2 g of samples and CRMs were weighed into a covered PTFE beaker. A volume of 5 mL of HCl was added dropwise and letting the reaction to diminish between additions. When the reaction has decreased, usually around two hours after, it was slowly added 2.5 mL of HF, taking care for the mixture temperature did not exceed 50 ºC and stayed overnight. Then, a volume of 3.5 ml of HNO_3 was added avowing heating of the mixture. After total decomposition, 8 ml of 50 g L^{-1} H_3BO_3 solution was added allowing the mixture to settle for two hours at least. The solution was transferred into a 50 ml volumetric flask and diluted to the mark with ultrapure water.

3 Results and Discussion

The measurand, mass fraction of each metal,w, in aluminum alloys, expressed in [g/(100g] was obtained by Eq. (1) taking into account the influencing factors and another potential sources due to the sample decomposition evaluated as recovery, R_γ.

$$w = \frac{10^{-4}.\gamma_M.V.\mathrm{F_{dil}}}{m.R_\gamma} \quad (1)$$

3.1 Analytical dynamic ranges

Atomic absorption spectrometric techniques require the comparison of the absorbance of the sample digestion solution with a set of calibration standard solutions. Table 2 shows both mass concentration and absorbance ranges of the calibration functions which are obtained by regression analysis after evaluation of linearity using Mandel fitting test [15–17] and assuming all errors normally distributed in y-axis. For Mg and Ti the second order function provide the best fit because the testing values, TV, were lower than the critical Fisher ones, F, while for Cr, Cu, Fe, Mn and Si linear calibration functions were used ($TV < F$), as shown in Table 2. In all situations the critical values of Fisher-Snedecor distribution was $F_{1;4;0.99} = 21.2$ and the squared correlation coefficients were higher than 0.998. Calibration quality coefficients, CQC, were calculated to assess the quality of regression analysis [17, 18] and CQC values from 0.01 to 0.03 (Table 2) were obtained confirming the adequacy of the calibration functions models since relative precision up to 0.05 is acceptable in FAAS [19, 20].

Limits of detection in the digestion solutions were calculated from both calibration blanks and residual standard deviations, as reported by Miller et al. [21], following IUPAC recommendations [22, 23] as previously discussed [9, 12, 17]. Table 2 reports the γ_{LOD} values showing the lowest concentration of the analytes that can be detected [24]. The γ_{LOQ} values give information about the lowest level of analyte that can be determined with the performance of the calibration curve. In this work γ_{LOQ} values were calculated considering the IUPAC default value of $k = 10$ [22–24], being $\gamma_{LOQ} = 3.3\gamma_{LOD}$ and they must be equal or lower than the lowest limit of the dynamic range. Table 2 shows that this requirement was always fulfilled. These limits depend on the precision of the regression and are checked using quality control standards.

For warranting the stability of the calibration functions throughout the analysis period, quality control standards solutions, every six sample sets, were analysed. No drift were considered whenever relative errors on γ_{QC} were within ± 0.05 of the expected values for FAAS with air-C_2H_2 flame or ± 0.10 in case of N_2O-C_2H_2 flame [11, 17] due to more flame instability. If γ_{QC} values were outside the measurements then a new calibration was carried out [11, 12, 17].

Table 3 shows s^{rel}_{QC} values obtained from the individual control charts. Target values of s^{rel}_{QC}, were defined considering the acceptance criteria defined and assuming a rectangular distribution. For Cr, Si and Ti the $s^{rel}_{QC(tg)}$ values of 0.058 and $s^{rel}_{QC(tg)} = 0.029$ for Cu, Fe, Mg, Mn and Zn were obtained.

3.2 Contaminations

In this work two blanks were produced: the calibration blank, B_c, and the digestion blank, B_{dig}, carried out in each acid digestion batch. These blanks allow the control of possible contamination resulting from either the reagents or the equipment used during sample processing. In routine analysis, B_c absorbance were accepted whenever $B_c \leq 0.005$ for Cr, Cu, Fe, Mn, Si, Ti, Zn and $B_c \leq 0.015$ for Mg. In case of digestion blanks, the B_{dig} absorbance criteria were

Table 3 Validation and quality report

Parameter	Range [g/(100 g)]	Precision			Trueness					
		s^{rel}_r	s^{rel}_{QC}	s^{rel}_{IP}	$\overline{R}_{CRM}$	$u\left(\overline{R}_{CRM}\right)$	t_{cal}	w_{LOQ} g/100 g	$u^{rel}_c(w)$	$u^{rel}_{c\_tg}(w)$
Cr	0.04–1.6	0.014	0.013	0.019	1.049	0.005	1.1	0.002	0.056	0.086
Cu	0.05–3	0.016	0.028	0.031	1.003	0.010	0.2	0.02	0.035	0.074
Fe	0.3–1	0.022	0.042	0.044	1.002	0.006	0.1	0.11	0.048	
Mg	0.1–2.5	0.030	0.023	0.036	0.974	0.013	2.0	0.003	0.040	
Mn	0.004–0.3	0.028	0.024	0.037	0.988	0.009	0.21	0.002	0.066	
Si	0.1—8	0.020	0.021	0.029	0.996	0.013	0.21	0.15	0.034	0.086
Ti	0.01–0.1	0.034	0.053	0.063	0.960	0.012	1.6	0.26	0.064	
Zn	0.02–2.1	0.018	0.018	0.026	0.986	0.030	0.8	0.002	0.042	0.074

s^{rel}_r given by Eq. (2), $\overline{R}_{CRM}$ given by Eq. (6), $u\left(\overline{R}_{CRM}\right)$ given by Eq. (7), t_{cal}calculated t statistic [25], $u^{rel}_c(w)$ given by Eq. (8), $u^{rel}_{c\_tg}(w)$ given by Eq. (8)

$B_{dig} \leq 0.005$ for Cr, Fe, M and Si, $B_{dig} \leq 0.020$ for Mg and $B_{dig} \leq 0.010$ for Cu and Zn. These limits are the warning limits of individual control charts. Additionally $\left|B_{dig} - B_c\right| \leq 0.003$. Otherwise, new calibration curves were calculated using the CS absorbance after subtracting the B_c values. In such cases γ_M values were recalculated using the absorbance deducted from the B_{dig} value (1716).

3.3 Matrix effects

The assumption that no matrix effect in calibration function due to the matrix difference between calibration solutions and digestion solutions was evaluated by spiking digestion solutions with known amounts of analyte. Whenever the target recovery is inside the interval (1.00 ± 0.10) that requirement is fulfilled. As can be seen in Table 3 no matrix effects were found for Cr (F_{dil}= 1), Cu ≥ (F_{dil}50), Mn ($F_{dil} \geq 10$); Mg ($F_{dil} \geq 10$), Si (F_{dil}= 1) and Zn ($F_{dil} > 50$) because target recoveries were fulfilled and = R_γ1 could be used in Eq. (1). Otherwise matrix effects were found for Fe (F_{dil} =25), Mg (F_{dil} =2.5), Mn ($F_{dil} \leq 10$) and Ti (F_{dil} =1) and $\overline{R}_\gamma$ values used in Eq. (1) were those reported Table 4.

3.4 Precision

Measurement repeatability of the overall procedure was estimated from duplicate analysis of aluminum alloys, which instrumental signal was higher than γ_{LOQ} values and s_r^{rel} given by Eq. (2).

$$s_r^{rel} = \frac{s\left(A_j^{rel}\right)}{\sqrt{2}} \tag{2}$$

A target relative standard deviation was stated based on the relative acceptance criterion of 0.10 for amplitude ranges and taking into account the definition of limit of repeatability for duplicated sets at a coverage probability of approximately 95% [26]. In this conditions $s_r(tg)^r el = 0.1/2.8 = 0.04$. Table 4 presents duplicate ranges and s_r^{rel} values, which are adequate to the intended use of the results because $s_r^{rel} \leq s_{r(tg)}^{rel}$.

Intermediate measurement precision expressed as relative standard deviation, s_{IP}^{rel}, was estimated by Eq. (3), which associates s_r^{rel} values, over a large mass fraction ranges, with s_{QC}^{rel} values obtained as described in 3.1.

$$s_{IP}^{rel} = \sqrt{\left(s_r^{rel}\right)^2 + \left(s_{QC}^{rel}\right)^2} \tag{3}$$

Target for s_{IP}^{rel} and $s_{IP(tg)}^{rel}$, were also stated using Eq. (3) considering the corresponding ones. So, $s_{IP(tg)}^{rel} = 0.068$ for Cr, Si and Ti and $s_{IP(tg)}^{rel} = 0.046$ for Cu, Fe, Mg, Mn and Zn were obtained. From Table 2 all target values were fulfilled.

3.5 Trueness

The comparison of the obtained measurement CRM values with the certified ones follows the application note 1 of the European Reference Materials [25]. In this approach the difference $\Delta = \left|w_{CRM} - \overline{w}_{CRM}^{obs}\right|$, was compared with U_Δ given by:

$$U_\Delta = 2\sqrt{u\left(w_{CRM}\right)^2 + u\left(\overline{w}_{CRM}^{obs}\right)^2} \tag{4}$$

Standard uncertainty of w_{CRM} reported in the NIST SRM 87a certificate has no information about the coverage factor, k. So, $k = 1$ was used. Once none of $u\left(w_{CRM}\right)$ values reported were available for BCS 181/1 it was adopted those from the certificate of the BCS 181/3, dated of 2013. In case of BCS Nº 268 and Nº 300 $u\left(w_{CRM}\right)$ values were calculated by Eq. (5) because those certificates only report the individual results of participants. The Eq. (5) was also used to obtain $u\left(\overline{w}_{CRM}^{obs}\right)$ values from experimental values. As shown in Table 5, in all situations $< \Delta < U_\Delta$ for a confidence level of around 0.95 and no significant differences among the measurement results and the certified values were found.

$$u\left(w_{CRM}\right)\frac{s}{\sqrt{n}} \tag{5}$$

Mean recovery from CRM analysis was calculated by Eq. (6) while $u\left(\overline{R}\right)$, by Eq. (7), because CRM analysis was performed on intermediate precision conditions

Table 4 Spike recoveries for matrix influence on atomic absorption measurements

Element	F_{dil}	Spike (mg L^{-1})	$\overline{R}_\gamma \pm s$
Chromium	1	0.5 and 1.0	0.974 ± 0.003
Copper	50 and 250	0.2 and 0.4	0.996 ± 0.032
Iron	25	0.5 and 1.0	0.891 ± 0.016
Magnesium	2.5	0.05 and 0.1	0.731 ± 0.014
	10	0.05 and 0.1	0.101 ± 0.020
Manganese	25	0.1	0.101 ± 0.021
	10; 5 and 2	0.2	0.838 ± 0.022
Silicon	1	10 and 20	0.975 ± 0.082
Titanium	1	5 and 10	0.779 ± 0.021
Zinc	625	0.05 and 0.1 0.125 and 0.25	0.960 ± 0.024

$\overline{R}_\gamma = \left(\gamma_{M+sp} - \gamma_{sp}\right)/\gamma_{sp}$

Table 5 Comparison of measurement results with the certified values

Elements	CRM	w_{CRM}	$u(w_{CRM})$	$\overline{w}^{obs}_{CRM}$	$u\left(\overline{w}^{obs}_{CRM}\right)$	Δ	$U(\Delta)$
Cr	SRM 87a	0.11	0.01	0.12	0.003[b]	0.006	0.02
	BCS N.º 300	0.15	0.003	0.16	0.005[b]	0.007	0.01
Cu	SRM 87a	0.30	0.01	0.30	0.01[a]	0.003	0.02
	BCS-CRM N.º 181/1	3.99	0.027	3.93	0.08[a]	0.06	0.18
	BCS n.º 268	1.34	0.006	1.37	0.05[b]	0.03	0.10
	BCS N.º 300	1.28	0.007	1.30	0.03[a]	0.02	0.06
Fe	SRM 87a	0.61	0.02	0.60	0.02[b]	0.01	0.06
	BCS-CRM N.º 181/1	0.36	0.004	0.35	0.01[a]	0.01	0.02
	BCS n.º 268	0.39	0.004	0.40	0.01[b]	0.01	0.03
	BCS N.º 300	0.30	0.004	0.31	0.01[b]	0.01	0.02
Mg	SRM 87a	0.37	0.01	0.37	0.01[a]	0.002	0.034
	BCS-CRM N.º 181/1	1.42	0.01	1.37	0.03[a]	0.05	0.06
	BCS n.º 268	0.56	0.01	0.53	0.01[a]	0.027	0.028
	BCS N.º 300	2.76	0.01	2.71	0.07[a]	0.05	0.15
Mn	SRM 87a	0.26	0.01	0.26	0.005[a]	0.004	0.022
	BCS-CRM N.º 181/1	0.10	0.002	0.10	0.001[a]	0.002	0.005
	BCS n.º 268	0.22	0.003	0.21	0.0004[a]	0.005	0.006
	BCS N.º 300	0.41	0.003	0.41	0.01[a]	0.003	0.022
Si	SRM 87a	6.24	0.03	6.29	0.06[a]	0.05	0.14
	BCS-CRM N.º 181/1	0.38	0.01	0.38	0.02[a]	0.001	0.043
	BCS n.º 268	4.85	0.02	4.77	0.06[a]	0.08	0.12
Ti	SRM 87a	0.18	0.010	0.18	0.002[a]	0.004	0.020
	BCS-CRM N.º 181/1	0.14	0.001	0.13	0.01[a]	0.009	0.012
	BCS N.º 300	0.15	0.002	0.15	0.003[a]	0.005	0.008
Zn	SRM 87a	0.16	0.01	0.16	0.003[a]	0.004	0.021
	BCS-CRM N.º 181/1	0.02	0.0001	0.02	0.001[a]	0.001	0.017
	BCS n.º 268	0.05	0.001	0.05	0.001[a]	0.0005	0.002
	BCS N.º 300	5.98	0.013	5.99	0.04[a]	0.011	0.078

[a] $\overline{w}^{obs}_{CRM}$ given by Eq. (5)
[b] $\overline{w}^{obs}_{CRM} = \frac{0.10\times\overline{w}^{obs}_{CRM}}{2\sqrt{3}}$; $U(\Delta)$ given by Eq. (4) for $k=2$; $p\sim0.05$

quantifying the combination of pure random effects with the variation between run systematic effects [10].

$$\overline{R}_{CRM} = \sum_{i=1}^{N} \frac{\overline{w}^{obs}_{CRM}}{w_{CRM}} \tag{6}$$

$$u\left(\overline{R}_{CRM}\right) = \frac{1}{N}\sqrt{\sum_{i=1}^{N}\left[R^2_{CRM}\left(\left(\frac{u\left(\overline{w}^{obs}_{CRM}\right)}{\overline{w}^{obs}_{CRM}}\right)^2 + \left(\frac{u\left(w_{CRM}\right)}{w_{CRM}}\right)^2\right)\right]} \tag{7}$$

Table 3 shows the mean recovery and $u\left(\overline{R}_{CRM}\right)$ values calculated using data of Table 5. Previously target values for recovery were defined considering the acceptance criteria: $0.90 \le R \le 1.00$. Using the t statistic significance test [24], as shown in Table 2, it can be established that mean recoveries of CRM analysis were metrologically equivalent to 1 for a level of confidence of approximately 95%, because $\le t_{cal}2$, being two the coverage factor [8]. Additionally a target value of 0.058 for $u\left(\overline{R}_{CRM}\right)$ can be considered taking into account the acceptance criteria and assuming a rectangular distribution.

3.6 Measurement uncertainty

Measurement uncertainty of the results was estimated combining precision and trueness uncertainty components. This model is based on the concept that accuracy comprises precision plus trueness and that relative combined standard uncertainty, $u_c^{rel}(w)$, comprises the two main components of uncertainty budget: intermediate precision and recovery according to Eq. (8) [8–10].

$$u_c^{rel}(w) = \sqrt{u\left(s_{IP}^{rel}\right)^2 + u\left(\overline{R}_{CRM}\right)^2} \quad (8)$$

Combining the target values of the uncertainty components of Eq. (8), reported before, target values for combined uncertainty were stated. For Cr, Si and Ti, $u_{c\_tg}^{rel} = 0.089$ and for Cu, Fe, Mg, Mn and Zn = $u_{c_tg}^{rel}$0.074 were obtained. These two groups were differentiated because $s_{QC(tg)}^{rel}$ values were higher for N_2O-C_2H_2 flame than air-C_2H_2 one. Table 3 summarizes $u_c^{rel}(w)$ values for the alloying elements and the target ones were fulfilled.

The relative expanded uncertainty values were obtained multiplying $u_c^{rel}(w)$ (Table 6) by a coverage factor of 2, for a confidence level of approximately 95% [7].

Results of metals in aluminum alloys with the associated expanded uncertainty in non-ferrous fraction from auto-shredders, are shown in Table 5 as example, following the described validation and quality control actions, which assures confidence in both measurement procedures used and the results obtained.

4 Conclusion

In this work the analytical performance characteristics of the procedures were determined setting up validation and quality control actions in the characterization of the relevant alloying elements of aluminum alloys (Si, Mg, Cu, Zn, Mn, Ti, Fe and Cr). The results proved the approach of sorting aluminum alloys based on its chemical composition. Summarizing: two different acid digestion mixtures were used: an HCl-HNO_3 acid mixture for Mg, Cu, Zn, Mn, Ti, Fe and Cr analysis and HCl-HNO_3-HF mixture followed by HF complexation using H_3BO_3 for silicon due to the chemical behaviour of silicon; linear calibration function for Cr, Cu, Fe, Mn, Si, Zn and second order function for Mg and Ti were defined using Mandel fitting test; stability of calibration functions performance over the analysis as QC warranted by the fulfilling of the target relative errors for γ_{QC} within ± 0.05 of the expected values for Cu, Fe, Mg, Mn and Zn (air-C_2H_2 flame) and ± 0.10 for Cr, Si and Ti (N_2O-C_2H_2 flame); matrix difference between the acid digestion solutions and CS were not found for Cr, Cu, Mn, Mg, Si and Zn ($R_\gamma = 1$), while for Fe (F_{dil} =25), Mg (F_{dil} =2.5), Mn ($F_{dil} \leq 10$) and Ti (F_{dil} =1) $\overline{R}_\gamma$ values used are those reported in Table 4; repeatability from duplicates were adequate to purpose because $s_r^{rel} \leq s_{r(tg)}^{rel}$ (Table 4); no bias were found from CRM´s analysis (Tables 4 and 5) and measurement uncertainty of the results was estimated combining overall precision and trueness uncertainty components based on the concept that accuracy combines these two components.

Table 7 shows the typical mass fraction ranges of the discriminating elements of the most common Al wrought and cast alloys, by series. Silicon was the element that allows the differentiation between cast and wrought alloys. In case of cast alloy silicon discriminates series 400 with highest mass fractions. The only wrought alloys having high Si mass fractions are the 4000 series, but these are rarely found.

For wrought alloys manganese is the discriminating element for series 3000 while for series 5000 it is also Mg. For series 6000 only Mg is relevant, but with lowest levels than 5000 ones, while for series 7000 is Mg and Zn. Series 1000 has low content of all alloying elements. The adequacy of the procedures to the low mass fractions were evaluated using the uncertainty information in compliance assessment [28]. For instances for silicon the w_{LOQ} values is 0.15 g/100 g (Table 3), which fulfills the compliance with the upper limit of 0.2 g/100 g (Table 7) because these value is lower than the acceptance limit of 0.19 g/100 g calculated as $[0.2–1{,}65 \times u_c]$ being 1,65 the one tailed t value at 95% confidence and u_c given in Table 3. The same is true when comparing the w_{LOQ} values (Table 3) with the calculated acceptance limits for Mg, Cu and Zn of (0.19 g /100 g) and 0.18 g /100 g for Mn, which also shows that the

Table 6 Mass fraction composition of aluminum alloys of non-ferrous fraction of auto-shredders

Parameter	Range [g/(100 g)]	$w \pm U(w)$, [g/(100g]			
		Sample 1	Sample 2	Sample 3	Sample 4
Cr	0.04–1.6	0.0921 ± 0.010	0.0389 ± 0.0044	0.0152 ± 0.0017	0.0179 ± 0.0020
Cu	0.05– 3	0.161 ± 0.011	2.95 ± 0.21	2.51 ± 0.18	0.220 ± 0.015
Fe	0.3–1	0.250 ± 0.024	0.927 ± 0.089	0.914 ± 0.088	0.941 ± 0.090
Mg	0.1–2.5	0.562 ± 0.045	0.126 ± 0.010	0.335 ± 0.027	0.191 ± 0.015
Mn	0.004– 0.3	0.0695 ± 0.0092	0.310 ± 0.041	0.178 ± 0.023	0.190 ± 0.025
Si	0.1–8	0.423 ± 0.029	7.27 ± 0.49	9.62 ± 0.65	12.25 ± 0.83
Ti	0.01–0.1	0.0248 ± 0.0032	0.0608 ± 0.0078	0.0449 ± 0.0058	0.0271 ± 0.0035
Zn	0.02–2.1	0.0147 ± 0.0012	0.865 ± 0.073	1.19 ± 0.10	0.276 ± 0.023

w mass fraction given by Eq. (1), $U(w)$ expanded uncertainty of w, ($k = 2; p \sim 0.95$)

Table 7 Typical mass fractions of most common Al wrought alloys and Al cast alloys, by alloy series (series designation according with the International Alloy Designation System—IADS

	Series	Si		Mg		Cu		Mn		Zn		Obs. and frequency in non-ferrous scrap
		Min	Max	Min	Max	Min	Max	Min	Max	Min	Max	
Wrought alloy	1000	< 0.2		< 0.2		< 0.2		< 0.2		< 0.2		> 99.5% Al (low contents of other metals) Very frequent
	3000							0.3 (U = 0.040)	1.5 (U = 0.20)			Very frequent
	5000			1 (U = 0.080)	5 (U = 0.40)			n.d	0.8 (U = 0.11)			Very frequent
	6000	0.5 (U = 0.034)	2 (U = 0.14)	0.5 (U = 0.040)	1 (U = 0.080)							Very frequent
	4000	5 (U = 0.34)	12 (U = 0.82)									Rarely found in scrap
	7000			2 (U = 0.16)	3 (U = 0.24)					1 (U = 0.084)	7.6 (U = 0.64)	Less frequent
Cast alloy	300	5 (U = 0.34)	15 (U = 1.0)			n.d	4.5 (U = 0.32)					Most frequent
	400	5 (U = 0.34)	12 (U = 0.82)									Less frequent
	200					2 (U = 0.14)	4.5 (U = 0.32)					Rarely found in scrap

Most 300 alloys have copper content higher than 1%, thus easily differentiated from 400 alloys. However, some alloys from 300 series can have low Cu content, which can be hard to discriminate from 400 series

procedures and both quality control actions and targets used were adequate for these elements.

In case of cast alloy series 200 copper is the discriminating and for series 300 is Si and Cu.

Measurement uncertainty gives the quality of the result and defines the numerical expression of results. If expanded uncertainty is given, no more than two significant digits for reporting uncertainty is recommended and the results should be rounded to be consistent with the provided uncertainty. As can be seen from Tables 6 and 7, with the U values reported becomes clear that the figures of the limit values are not affected by uncertainty.

The results obtained in this investigation were very useful for design of the separation devices within the Shreddersor project, and we believe it will also be quite relevant for the scrap recycling industry, at various levels, in the perspective of the application of the sorting operations to aluminum alloy fragments: (a) firstly, the possibility of accurately analyzing the main alloying elements is demonstrated, with the proposed procedures, in order to identify the main alloys present in the scrap, allowing the stakeholders to have reliable information on the materials they deal with; secondly, it will also allow recyclers to design and operate sorting operations according with the material feed, to identify precisely the separated alloys, and to quantify the separation efficiencies and the purity of the fractions they produce.

Acknowledgements The work here presented is included in the European project ShredderSort (Grant Agreement Nr. 603676, FP7 Theme ENV.2013.6.3-1; ENV.2013.6.2-3, collaborative projects). The authors wish to acknowledge the financial support of the European Commission. The authors acknowledge Jorgiana Branco from LNEG for providing the digestion procedures during the research.

Compliance with ethical standards

Conflict of interest The authors declare that they have no competing interests.

References

1. Margarido F, Nogueira CA, Novais Santos R, Durão F, Guimarães C; Trancoso MA, Oliveira PC, Pedrosa F, Gonçalves AM (2015) Evaluation of main aluminum alloys in non-ferrous fraction of auto-shredder recycling process, in M2D2015-6th International conference on mechanics and materials in design (Proc), Ponta Delgada, Açores, Portugal, 2015, J. F. Silva Gomes, S. A. Meguid, (Eds), 2033–2038
2. Nogueira CA, Trancoso MA, Pedrosa F, Crujeira AT, Oliveira PC, Gonçalves AM, Margarido F, Novais Santos R, Durão F, Guimarães C (2015) The role of automated sorting in the recovery of aluminum alloys waste. In: Vilarinho C, Castro F, Russo M (eds) WASTES: Solutions, Treatments and Opportunities. CRC Press-Taylor & Francis, London, UK
3. Hatayama H, Daigo I, Matsuno Y, Adachi Y (2012) Evolution of aluminum recycling initiated by the introduction of next-generation vehicles and scrap sorting technology. Resour Conserv Recy 66:8–14
4. Flame Atomic Absorption Spectrometry, Analytical Methods, Fourteenth edition, Agilent Technologies Australia (M) Pty, Ltd. (2017) https://www.agilent.com/cs/library/usermanuals/public/0009.pdf Accessed 02 mar 2018
5. Teixeira P, Calisto S, Lopes H (2015) Trancoso MA. Accred Qual Assur 20:67–74
6. Joint Committee for Guides in Metrology (2012) International vocabulary of metrology - basic and general concepts and associated terms (VIM). BIPM, Sèvres
7. ISO 11352 (2012) Water quality–estimation of measurement uncertainty based on validation and quality control data. International Organization for Standardization, Geneva, CH
8. Barwick VJ, Ellison SLR (2000) VAM project 3.2.1–part (d) protocal for uncertainty evaluation data. LGC, London
9. Trancoso I, Roseiro LB, Martins PL, Trancoso MA (2009) Validation and quality assurance applied to goat milk chemical composition: Minerals and trace elements measurements. Dairy Sci Technol 89:241–256
10. Cordeiro RMS, Rosa CMG, Silva RJNB (2018) Measurements recovery evaluation from the analysis of independent reference materials: analysis of different samples with native quantity spiked at different levels. Accred Qual Assur 23:57–71
11. Alves S, Correia dos Santos MM, Trancoso MA (2009) Accred Qual Assur 14:87–93
12. Trancoso MA, Sousa A, Mouro F, Freitas MC, Almeida S, Canha N (2012) Accred Qual Assur 17:199–206
13. Thermo Fisher Scientific (2008) Atomic Absorption Spectrometry Methods Manual, 9499 400 30011, Issue 5
14. American Public Health Association (APHA) (2017) Standard methods for the examination of water and wastewater, 23rd edn. American Public Health Association, Washington, DC
15. ISO 8466–1 (1990) Water quality - Calibration and evaluation of analytical methods and estimation of performance characteristics. Part 1: Statistical evaluation of the linear calibration function. International Organization for Standardization Geneva, CH
16. ISO 8466–2 (2001) Water quality - Calibration and evaluation of analytical methods and estimation of performance characteristics - Part 2: Calibration strategy for non-linear second-order calibration functions. International Organization for Standardization, Geneva, CH
17. Trancoso MA, Correia dos Santos MM, Gonçalves MLS (2003) Quality assurance program for the chemical characterization of soils. Accredit Qual Assur 8:323–333
18. Subramanian G (ed) (1995) Quality Assurance in environmental monitoring – instrumental methods. New York, VCH, Weinheim
19. Welz B, Sperling M (1999) Atomic absorption spectrometry. Wiley_VCH, Weinheim
20. OTTO M (1998) Multivariate methods. In: Kellner R, Mermet JM, Otto M, Widmer HM (eds) Analytical chemistry. Wiley-VCH, Weinheim
21. Miller J, Miller J (2005) Statistics and chemometrics for analytical chemistry, 5th edn. Pearson, London
22. IUPAC (1978) Nomenclature symbols units and their usage in spectrochemical analysis–II. Spectromchim Acta. https://doi.org/10.1016/0584-8547(78)80043-3
23. Currie LA (1995) Nomenclature en evaluation of analytical methods, including detection and quantification capabilities (IUPAC recommendations 1995). Pure Appl Chem 67:1699–1723
24. F. B. Magnusson and U. Örnemark (eds.) Eurachem Guide: The fitness for purpose of analytical methods – a laboratory guide to method validation and related topics, (2nd ed. 2014). ISBN

978–91–87461–59–0. Available from https://www.eurachem.org Accessed 12 jan 2018
25. Linsinger T (2005) Comparison of a measurement result with thecertified value, application note 1. European reference materials, Geel. https://ec.europa.eu/jrc/sites/defaul Accessed 12 jan 2018
26. ISO 5725–1 (1994) Accuracy (trueness and precision) of measurement methods and results–part 1 General principles and definitions. ISO, Geneva
27. Eurachem/CITAC Guide (2012) Quantifying uncertainty in analytical measurement, 3rd edn. In: Ellison SRL, Williams A (eds).ISBN: 978–0–948926–30–3. https://www.eurachem.org. Accessed 12 jan 2018
28. S L R Ellison and A Williams (Eds). Eurachem/CITAC guide: Use of uncertainty information in compliance assessment. (First Edition (2007). Available from www.eurachem.org." Accessed 22 jun 2020